

# PHYSICAL REVIEW D

## PARTICLES AND FIELDS

THIRD SERIES, VOLUME 32, NUMBER 5

1 SEPTEMBER 1985

### Study of $D^*$ production in high-energy $\gamma p$ interactions

K. Sliwa, J. A. Appel, J. Biel,<sup>(a)</sup> D. Bintinger,<sup>(b)</sup> J. Bronstein,<sup>(a)</sup> C. Daum,<sup>(c)</sup> P. M. Mantsch,  
T. Nash, M. V. Purohit, W. Schmidke,<sup>(d)</sup> M. D. Sokoloff, W. J. Spalding, K. C. Stanfield,  
M. Streetman, and S. E. Willis<sup>(e)</sup>

*Fermi National Accelerator Laboratory, Batavia, Illinois 60510*

V. K. Bharadwaj,<sup>(f)</sup> B. H. Denby, A. M. Eisner,<sup>(g)</sup> R. G. Kennett,<sup>(h)</sup> A. Lu, R. J. Morrison, D. J. Summers,  
M. S. Witherell, and S. J. Yellin

*University of California at Santa Barbara, Santa Barbara, California 93106*

P. Estabrooks and J. Pinfold

*Carleton University, Ottawa, Canada K1S 5B6*

D. F. Bartlett, S. Bhadra, A. L. Duncan,<sup>(i)</sup> J. R. Elliott, and U. Nauenberg

*University of Colorado, Boulder, Colorado 80309*

M. J. Losty

*National Research Council of Canada, Ottawa, Ontario, Canada K1A 0R6*

G. R. Kalbfleisch and M. Robertson<sup>(j)</sup>

*University of Oklahoma, Norman, Oklahoma 73019*

D. E. Blodgett, S. B. Bracker, G. F. Hartner, B. R. Kumar, G. J. Luste, J. F. Martin, K. K. Shahbazian  
R. A. Sheperd, and C. J. Zorn

*University of Toronto, Toronto, Canada M5S 1A7*

(Received 17 September 1984)

We have studied  $D^*$  production mechanisms using data from a photoproduction experiment at the Fermilab Tagged Photon Spectrometer. A large sample of charged  $D^*$ 's was selected via the clean signature of the cascade decay  $D^* \rightarrow D^0 \pi^+$  and subsequently  $D^0 \rightarrow K^- \pi^+$  or  $D^0 \rightarrow K^- \pi^+ \pi^0$ . The cross section for the process  $\gamma p \rightarrow (D^{*+} + \text{anything})p$  at an average energy of 105 GeV was measured to be  $88 \pm 32$  nb. Only  $(11 \pm 7)\%$  of  $D^*$ 's were found to be consistent with being accompanied solely by a  $\bar{D}^*$  or a  $\bar{D}$ ; the remaining events contain additional particles. The distribution of the production angle of the  $D^*$  in the photon-fragmentation-system center of mass is strongly anisotropic and consistent with the form  $f(\theta^*) = \cos^4 \theta^*$ . We set a limit on the associated-production-process cross section  $\sigma(\gamma p \rightarrow (\bar{D}^{*-} + \text{anything})\Lambda_c) < 60$  nb (90% C.L.).

The photoproduction of charm particles can be viewed as a fluctuation of a photon into a  $c\bar{c}$  pair with subsequent scattering of one of the quarks off the target.<sup>1,2</sup> The framework of QCD can be applied to this process with the lowest-order perturbation-theory approximation considered to be adequate.<sup>1-6</sup> This is justified by the fact that the threshold invariant mass  $M_{\text{th}}^2$  of the produced charm system is large enough so that the effective QCD coupling constant  $\alpha_s(M_{\text{th}}^2)$  is small (0.2-0.4). Comparing the results from photoproduction experiments with models based on these ideas provides a valuable insight

into QCD, testing at least the validity of the lowest-order perturbation-theory approach. The existing data on the  $J/\psi$  photoproduction cross section agree very well with the calculations based on the photon-gluon fusion diagram.<sup>7-10</sup> There exist hardly any data, however, on variables describing directly photoproduced open-charm systems, especially those defined in the  $c\bar{c}$  (photon-fragmentation) center of mass. This paper presents distributions of several such variables which are measured directly for events with a single proton in the target-fragmentation system.

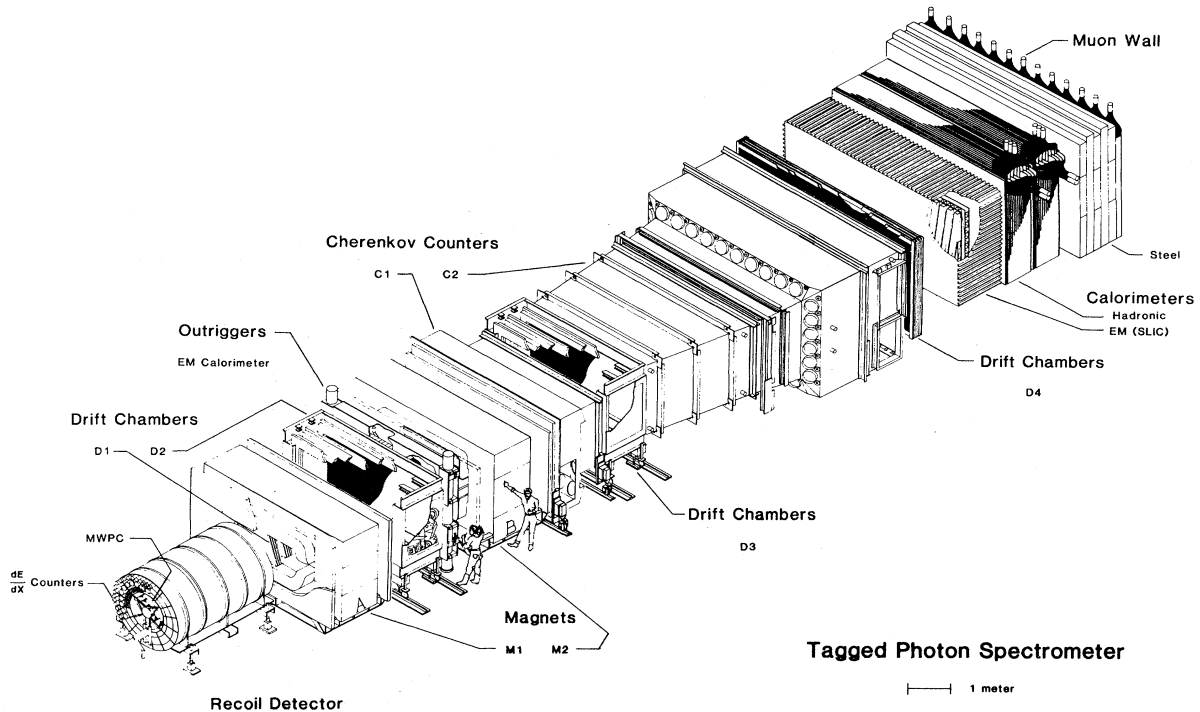


FIG. 1. The Tagged Photon Spectrometer at Fermilab.

The Fermilab Tagged Photon Spectrometer (TPS), described in detail elsewhere,<sup>11</sup> is unique in combining a large-acceptance, complete forward spectrometer with a sophisticated recoil detector. Together with a 1.5-m liquid hydrogen target, the system allows a complete measurement of four-momenta of initial ( $E_\gamma$ , proton target) and final-state (large-acceptance recoil and forward measurement) particles. This permits careful study of the mechanisms involved in photoproduction and decay of charm particles.<sup>12,13</sup> Here we present results of an analysis of  $D^*$  production based on data taken with the TPS. Photons, produced via the bremsstrahlung of 170-GeV electrons, had energies in the range  $40 < E_\gamma < 160$  GeV, with an average of 105 GeV. The integrated photon flux corresponds to a luminosity of  $480 \text{ nb}^{-1}$ .

The TPS detector is shown in Fig. 1. Twenty-nine planes of drift chambers and two large-aperture magnets were used to analyze forward charged tracks. Two unpressurized segmented Cherenkov counters (containing  $\text{N}_2$  and a  $\text{N}_2$ -He mixture) allowed charged-particle identification in the momentum range  $6\text{--}36 \text{ GeV}/c$  [ $\pi$  vs ( $K$  or  $p$ ) in the momentum range  $6\text{--}20 \text{ GeV}/c$ , and  $\pi$  vs  $K$  vs  $p$  between 20 and  $36 \text{ GeV}/c$ ]. Three high-resolution segmented electromagnetic shower detectors<sup>14</sup> were used for  $\pi^0$  detection. A hadron calorimeter<sup>15</sup> and a set of scintillator hodoscopes downstream of an iron filter used for muon identification completed the forward spectrometer system. The recoil detector<sup>16</sup> surrounding the liquid hydrogen target consisted of three cylindrical multiwire proportional counters (MWPC's) and a four-layer scintillator calorimeter in 15 azimuthal sectors covering 94% of  $2\pi$ .

It measured trajectories and energies of recoiling tracks. The detector accepted tracks with polar angle  $\theta > 20^\circ$  and momentum transfer in the range  $0.06 < |t| < 1.2$  ( $\text{GeV}/c$ )<sup>2</sup>. Energy resolution was 5–10% in this range. It also identified particle type ( $\pi$  vs  $p$  vs  $e$ ).

The geometrical acceptance in the laboratory frame for the recoil and forward systems, in terms of pion rapidity, is shown in Fig. 2. In the case of single-recoil-proton events, the recoil detector covered fully the target-fragmentation region and the forward spectrometer covered the photon-fragmentation region. A high-speed ECL-CAMAC trigger processor<sup>17</sup> attached to the recoil

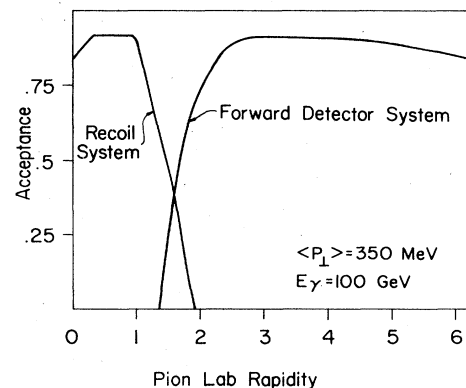


FIG. 2. TPS laboratory rapidity acceptance for the recoil and forward detector systems. Calculated for pions assuming  $\langle p_t \rangle = 350 \text{ MeV}/c$ ,  $E_\gamma = 100 \text{ GeV}$ .

system was designed to isolate two selected subclasses of the total-charm cross section. The "high-mass diffractive" trigger required a single proton at the primary vertex recoiling off the forward system with forward missing mass  $M_X > 2.0$  GeV.

We studied two possible sources of contamination in this trigger: events which had additional, unreconstructed tracks in the recoil system, and events in which a proton from a secondary interaction was associated with the primary vertex. Both classes of background events tend to mimic a high missing mass. The most significant contamination comes from events in which neutral particle(s) accompanying a proton remained undetected in the recoil detector. To investigate this problem we have constructed a model in which we assumed 30% of total photoproduction cross section to proceed via  $\gamma p \rightarrow XN^*$ ,  $N^* \rightarrow p\pi^0$ , and  $N^* \rightarrow p\pi^0\pi^0$  (with branching ratios of 60% and 40%, respectively). The four-momentum-transfer distribution was assumed to be of the form  $\exp(-3.5|t|)$  and the distribution of forward mass  $M_X$  flat in  $M_X^2$  from the pion threshold to 10 GeV. These Monte Carlo studies, which include the effects of detector inefficiencies, indicate that the contamination is vastly reduced for charm events with a single proton in the recoil. Observation of a  $D^*$  in such an event implies the pair-production process, and the mass of the forward system  $M_X > 4$  GeV. For this class of events the contamination was found<sup>18</sup> to be small,  $< 10\%$  even in the highest-mass bins, and does not affect the results shown.

The "target-fragmentation" trigger, optimized for  $\Lambda_c$  acceptance by means of a Monte Carlo study, required at

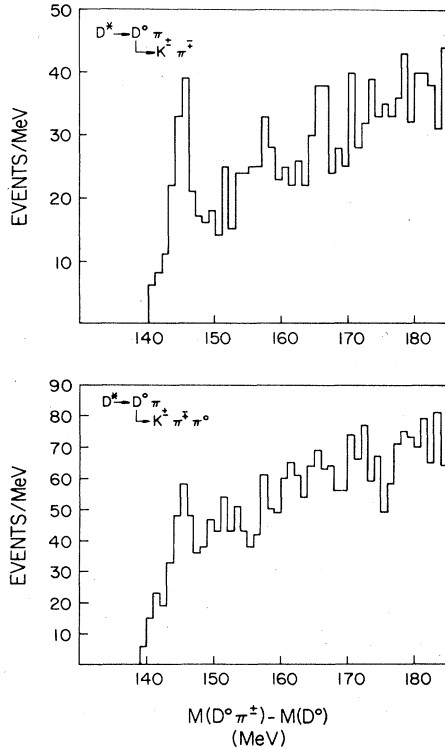


FIG. 3.  $D^*-D$  mass-difference histograms.

least three charged tracks (from the primary vertex) in the recoil detector.

For the present analysis we select a sample of charged  $D^*$  events in which a  $D^* \rightarrow D^0\pi^+$  decay was followed by one of the decays  $D^0 \rightarrow K^-\pi^+$ ,  $D^0 \rightarrow K^-\pi^+\pi^0$ . (Unless specified, the charge-conjugate states are implicitly included). Our technique exploits the fact that the  $D^{*+}-D^0$  mass difference is only a few MeV larger than the pion mass. As a result, the distribution of the mass difference  $M(D^0+\pi^+)-M(D^0)$  shows a clean, narrow peak at the  $D^*-D^0$  mass difference. We consider  $K^-\pi^+(\pi^0)$  combinations whose reconstructed invariant masses lie within 50 MeV of the  $D^0$  mass, 1865 MeV. We have used information from Cherenkov counters to assign each particle a set of particle-type probabilities ( $e, \mu, \pi, K, p$ ). For the multiparticle combinations the cuts used were on the joint probability for a given mass hypothesis.

For each  $K^-\pi^+(\pi^0)\pi^+$  combination we plot the mass difference

$$\Delta M = M_{K^-\pi^+(\pi^0)\pi^+} - M_{K^-\pi^+(\pi^0)}$$

Shown in Fig. 3, both channels in these plots manifest a strong  $D^*$  peak. Fitting the data to a background of the form  $aQ^{1/2}(1-bQ)$ , where  $Q = \Delta M - M_\pi$ , plus a Gaussian centered at the  $D^{*+}-D^0$  difference, 145.5 MeV ( $\sigma = 1.2$  MeV), gives  $64 \pm 12$   $D^0 \rightarrow K^-\pi^+$  events in the  $D^*$  peak and  $95 \pm 15$  in the  $K^-\pi^+\pi^0$  mode.

Restricting the sample to single-recoil-proton events, those in which a proton and no other track from the primary vertex has been reconstructed off-line in the recoil detector, we have measured the cross section for the recoil elastic process  $\gamma p \rightarrow (D^{*+} + \text{anything})p$ . (These events come from the high-mass diffractive trigger.) In the mode with  $D^0 \rightarrow K^-\pi^+$  we find  $34 \pm 8$  such events. After correction for the trigger and reconstruction efficiencies and assuming equal production rate for  $D^{*+}$  and  $\bar{D}^{*-}$  we obtain the cross section of  $85 \pm 21(\text{stat}) \pm 23(\text{syst})$  nb. For the  $K^-\pi^+\pi^0$  mode the corresponding numbers are  $36 \pm 11$  events and  $92 \pm 30 \pm 35$  nb. The corrections were determined using a full Monte Carlo simulation of the experiment.

The generated events were of the type  $\gamma p \rightarrow Xp$ , with the  $M_X$  distribution flat in  $M_X^2$  from charm-pair-production threshold to 12 GeV. The distribution of four-momentum transfer  $t$  to system  $X$  was assumed to be of the form  $\exp(-3.5|t|)$ . System  $X$  consisted of  $D^*\bar{D}^*$ ,  $D^*\bar{D}^*\pi^+\pi^-$ , and  $D^*\bar{D}^*\pi^+\pi^-\pi^0$  with adjustable relative frequencies.  $D^{*+}$  was allowed to decay into  $D^0\pi^+$  and, subsequently,  $D^0 \rightarrow K^-\pi^+$  or  $D^0 \rightarrow K^-\pi^+\pi^0$ . The anisotropy of  $D^*$  angular distribution in the c.m. of system  $X$  was an adjustable parameter, all other decays were generated according to isotropic phase space in the corre-

TABLE I. Energy dependence of the cross section.

Energy range (GeV)	$\sigma$ (nb)
40-80	$24^{+34}_{-24} \pm 8$
80-120	$98 \pm 31 \pm 32$
120-160	$105 \pm 39 \pm 33$

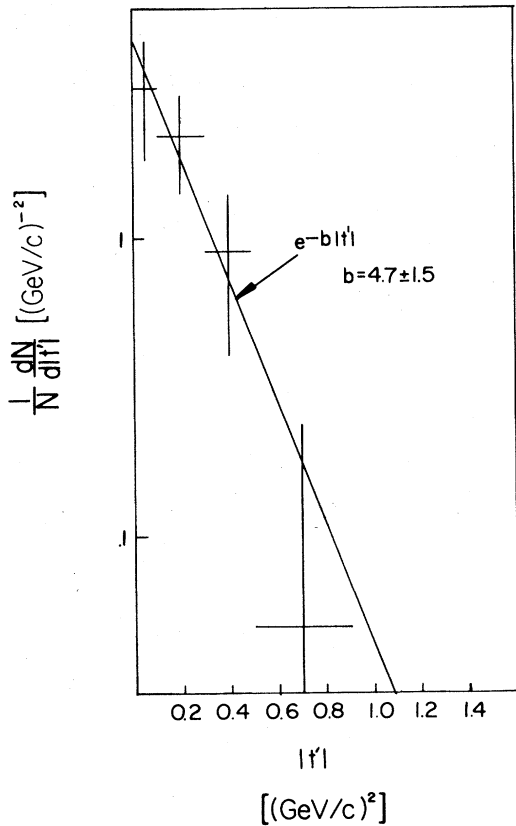


FIG. 4.  $t' = t - t_{\min}$  four-momentum-transfer distribution for single-recoil-proton events (efficiency and acceptance corrected).

sponding c.m. frames. The decay of the “other-side”  $\bar{D}^{*-}$  into  $D^0\pi$  was followed by  $D^0 \rightarrow K + n\pi$ , where decay modes and their ratios were adjusted to match results<sup>19</sup> of Mark II at the SLAC positron-electron ring on neutral- and charged-pion multiplicities of inclusive  $D^0$  decays. The generated particles were, after proper transformation into the laboratory frame, propagated through the complete simulation of the spectrometer.

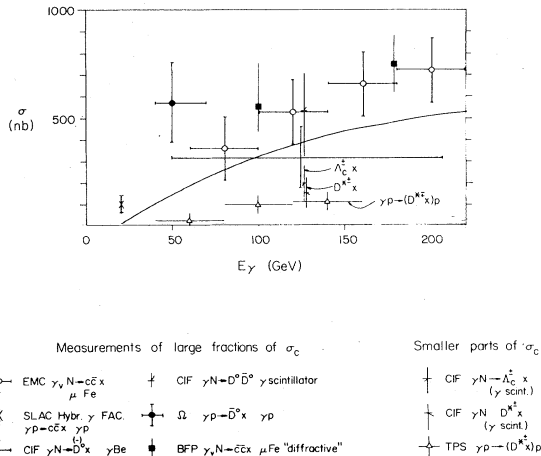


FIG. 5. Summary of charm-photoproduction cross-section measurements (Ref. 21).

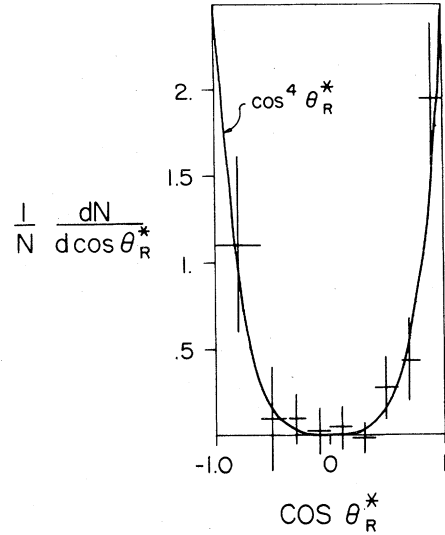


FIG. 6. Distribution of the  $D^*$  production angle in the photon-fragmentation system c.m. (acceptance and efficiency corrected).

The combined acceptance and detection efficiency for the  $D^0 \rightarrow K^- \pi^+$  and  $D^0 \rightarrow K^- \pi^+ \pi^0$  channels are  $0.164 \pm 0.010$  and  $0.041 \pm 0.003$ , respectively. [We have used branching ratios<sup>20</sup> of  $(2.4 \pm 0.4)\%$  and  $(9.3 \pm 2.8)\%$  for the  $D^0 \rightarrow K^- \pi^+$  and  $D^0 \rightarrow K^- \pi^+ \pi^0$ , respectively, and  $(64 \pm 11)\%$  for the  $D^* \rightarrow D^0 \pi^+$ .] Combining the two samples we find  $\sigma = 88 \pm 17 \pm 27$  nb. We have also measured the energy dependence of this cross section, as shown in Table I. This measurement is of what is often called the elastic or the diffractive part of the total  $D^*$  photoproduction cross section. This notion is supported by a sharp falloff in  $t' = t - t_{\min}$ , the four-momentum-transfer distribution measured using the target- and recoil-proton momenta. A background-subtracted  $t'$  plot of  $D^*$  data is shown in Fig. 4.

A summary of existing charm-photoproduction cross-section data<sup>21</sup> is presented in Fig. 5. Our cross-section measurement is  $\approx 20\%$  of the total-charm cross section

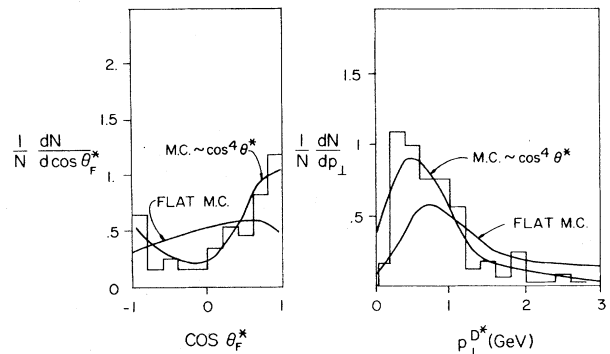


FIG. 7.  $\cos\theta_F^*$  and  $p_t$  for single-recoil-proton  $D^*$  events. Curves show Monte Carlo simulations for flat and  $\cos^4\theta^*$  dependence of the  $D^*$  production angle in the photon-fragmentation system c.m.

TABLE II.  $D^* p_t$  and  $\cos\theta_F^*$  for data and Monte Carlo.

	$\langle \cos\theta_F^* \rangle$	$\langle p_t^{D^*} \rangle$ (GeV/c)
Data	$0.25 \pm 0.06$	$0.75 \pm 0.04$
Monte Carlo:		
flat	0.08	1.44
$\cos^2\theta^*$	0.13	0.99
$\cos^4\theta^*$	0.23	0.80
$\cos^6\theta^*$	0.36	0.65

measured by the European Muon Collaboration<sup>8</sup> EMC and Berkeley-Fermlab-Princeton<sup>9</sup> (BFP). The direct ratio of the TPS ( $D^* + \text{anything}$ ) $p$  and Columbia-Illinois-Fermlab<sup>22</sup> (CIF)  $D^* + \text{anything}$  measurement is  $0.59 \pm 0.34$ . (Errors are dominated by the relative normalization uncertainties.) At the low end of the error range this is consistent with the elastic part being  $\approx 25\%$  of the total.

For the  $t'$  distribution and for all the distributions shown below that characterize  $D^*$  production, we have studied those events with  $\Delta M$  in the range 144–147 MeV. We have subtracted the background contribution estimated from the data by considering events which would have passed cuts except that either (a) the pion associated with the  $D^0$  combination was the wrong charge, (b)  $M_{K-\pi+(\pi^0)}$  was outside the  $D^0$  mass region (in 1.65–1.75 and 1.95–2.05 GeV), or (c)  $\Delta M$  was outside the  $D^*-D^0$  mass-difference region (in the 160–200-MeV range). The distributions from these three samples were combined and normalized to the amount of the background determined from the fit used for the cross-section measurement.

For the single-recoil-proton  $D^*$  events we have studied the angular distribution of the  $D^*$ 's in the c.m. of the photon-fragmentation system. We calculate the four-momentum of this system from the beam energy and the target- and recoil-proton momenta. We define  $\theta^*$  as the c.m. angle of the  $D^*$  with respect to the direction of the photon-fragmentation-system momentum in the laboratory ( $\theta^*$  is the polar angle of a  $D^*$  in the helicity frame).  $\theta^*$  can be measured in this experiment in two independent ways using recoil and forward detectors. The measurement derived from  $E_\gamma$ ,  $p_{\text{target}}$ , and  $p_{\text{recoil}}$  is called  $\theta_R^*$ . That derived by adding the four-momenta of observed

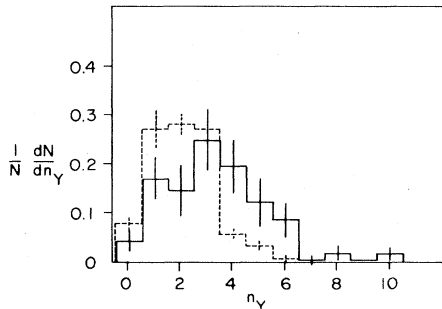


FIG. 8. Multiplicity of a system accompanying the observed  $D^* n_\gamma$ . Dashed line shows the expected distribution for  $D^* \bar{D}^*$  only events.

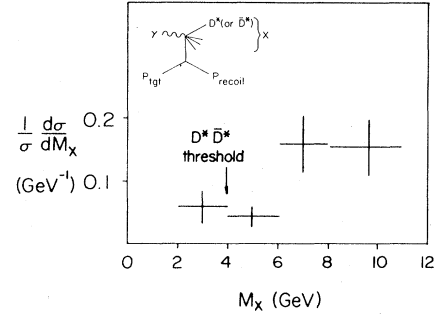
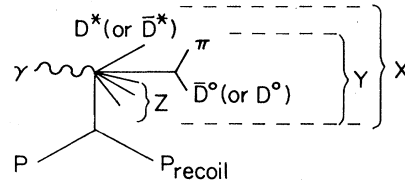


FIG. 9. Distribution of the mass of the photon-fragmentation system,  $M_X$ , for single-recoil-proton events with identified  $D^*$  (high-mass diffractive trigger). Efficiency and acceptance corrected, as are all the distributions presented below.

forward particles is called  $\theta_F^*$ . The  $\cos\theta_R^*$  distribution, corrected for the reconstruction efficiency, is shown in Fig. 6. It is strongly anisotropic and is consistent with the superimposed fitted distribution  $\cos^n\theta_R^*$ ,  $n = 4 \pm 1$ . In Fig. 7, we compare the data in distributions of other variables with Monte Carlo events generated with a  $\cos^4\theta^*$  and a flat  $\cos\theta^*$  distribution. Shown in Fig. 7 are  $p_t$  of the  $D^*$  and  $\cos\theta_F^*$ . The mean values of these two variables for the data and Monte Carlo samples with different  $\cos\theta^*$  distributions are listed in Table II.

Enhancement of forward-backward production in the case of photoproduction of heavy systems, as seen clearly in these distributions and measurements, was suggested by Bjorken.<sup>23</sup> The backward-going quark (antiquark) is "wee" in the laboratory and thus more likely to interact with the target. Based on scaling arguments, the model predicts a significant anisotropy of the angular distribution for large masses of the photon-fragmentation system,  $M_X$ . Similar anisotropy, expected to increase with the mass of the produced charm-anticharm system, is also predicted by the photon-gluon-fusion-model calculations (Bethe-Heitler process of QCD).<sup>24</sup>

As part of understanding how the  $c\bar{c}$  state hadronizes we have studied what accompanies the observed  $D^*$ . In the following diagram we define the three groups of outgoing forward particles ( $X$ ,  $Y$ , and  $Z$ ) that can be measured to give information on the forward state produced with the  $D^*$ :



$X$  represents all forward particles,  $Y$  is the forward system except the observed  $D^{*\pm}$ , and  $Z$  is the forward system exclusive of the observed  $D^*$  and a presumed but not directly observed  $D^*$ . Five essentially independent measurements are presented. These are the multiplicity of  $X$  and the masses of  $X$ ,  $Y$  (determined in two ways) and  $Z$ . All indicate that the  $D^*$  is rarely accompanied solely by a  $\bar{D}^*$  or a  $\bar{D}$ .

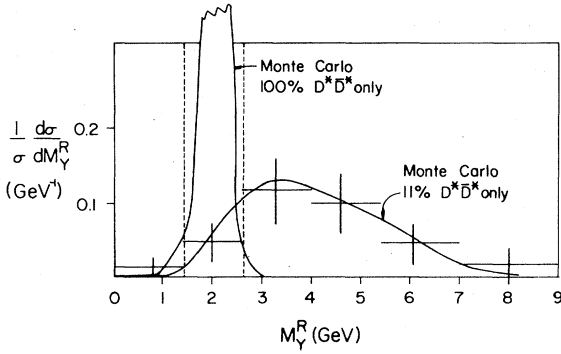


FIG. 10. Distributions of  $M_Y^R$  for single-recoil-proton events.

The observed multiplicity distribution of charged tracks in  $Y$ , for all  $D^*$  events with no secondary interactions is shown in Fig. 8. This is compared to what is expected if  $Y = \bar{D}^*$  only by using SPEAR Mark II and Lead Glass Wall data<sup>19</sup> smeared by the TPS detection efficiency (dashed line). The mean expected and observed multiplicities are  $\langle n_{\bar{D}^*} \rangle = 2.09 \pm 0.09$  and  $\langle n_Y \rangle = 3.20 \pm 0.26$ . The difference indicates the presence of at least one additional particle on average.

The distribution of  $M_X$  for the single-recoil-proton events with identified  $D^*$  is presented in Fig. 9. The turn on of  $D^*$  production is substantially higher than the  $D^*\bar{D}$  threshold suggesting the presence of additional particles.

The mass of the  $Y$  system, which should be about 2 GeV for  $D^*\bar{D}^*$  (or  $D^*\bar{D}$ ) only production can be measured in two independent ways. The most sensitive is the measurement made by calculating for single-recoil-proton events the missing mass  $M_Y^R$  of everything in the final state except the observed  $D^*$  and the recoiling proton. The distribution is shown in Fig. 10. The dashed lines at  $\pm 600$  MeV around 2 GeV include 95% of the Monte Carlo-generated distribution for  $D^*\bar{D}^*$  events, which peaks at the  $D^*$  mass. Only  $(11 \pm 7)\%$  of the data falls in this region. This is the strongest indication of the relative

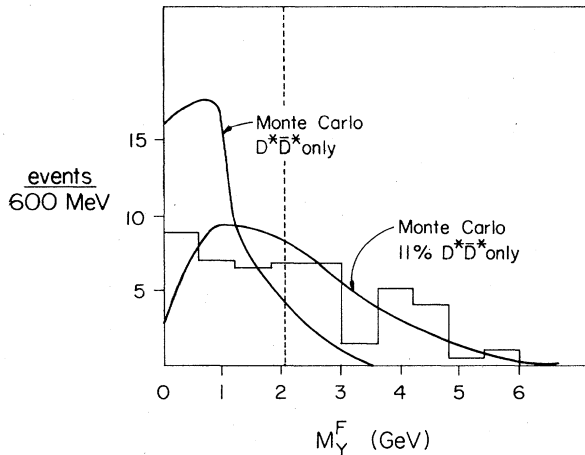


FIG. 11. Distributions of  $M_Y^F$ , computed directly from the observed charged and neutral particles.

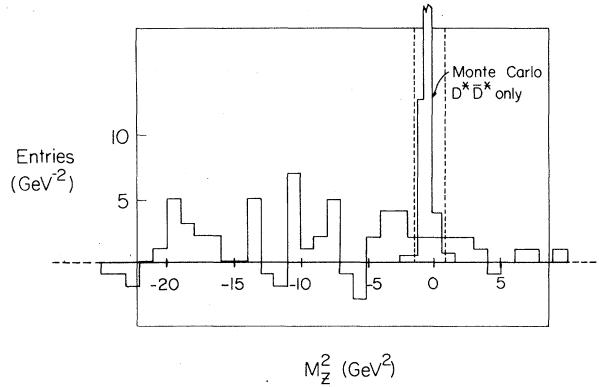


FIG. 12. Distributions of  $M_Z^2$  for single-recoil-proton events.

rarity of  $D^*\bar{D}^*$  or  $D^*\bar{D}$  only production. The solid curve shows the Monte Carlo expectation for 11%  $D^*\bar{D}^*$ , 44.5%  $D^*\bar{D}^*\pi^+\pi^-$ , and 44.5%  $D^*\bar{D}^*\pi^+\pi^-\pi^0$ . (Details of the Monte Carlo simulation are described earlier in the text.) Although this has excellent agreement with the data it is not intended to indicate that this distribution of extra particles is unique in matching the data. Channels with more than three  $\pi$ 's may contribute and cannot be confirmed or ruled out with this technique. A second way of measuring  $M_Y$  is to compute it directly from the observed charged and neutral particles. The distribution,  $M_Y^F$ , is shown in Fig. 11 for all  $D^*$  events with no secondary interactions. It gives the same conclusion as  $M_Y^R$  but because of detection inefficiencies is less sensitive. Here the fraction below 2 GeV (where 92% of Monte Carlo  $D^*\bar{D}^*$  events is contained) is  $(44 \pm 18)\%$ .

The fifth measurement assumes the presence of a second  $\bar{D}^*$  and computes  $M_Z$  of all particles in the forward system except the two  $D^*$ 's. For  $D^*\bar{D}^*$  only production  $M_Z = 0$ . The method is based on another consequence<sup>25</sup> of the small value of  $M_{D^*} - M_{D^0} - M_\pi$  (5.9 MeV). To a very good approximation the momentum of the  $D^*$  equals a constant times that of the  $\pi$  coming from  $D^* \rightarrow D^0\pi$  decay:  $P_{D^*} \approx 14.36 P_\pi$ . The energy of a  $D^*$  is then obtained by assuming the  $D^*$  mass.  $M_Z$  is computed for all available correct charge pions using the same approach as for the  $M_Y^R$  but here also subtracting the four momentum of the second  $D^*$ , obtained in the manner

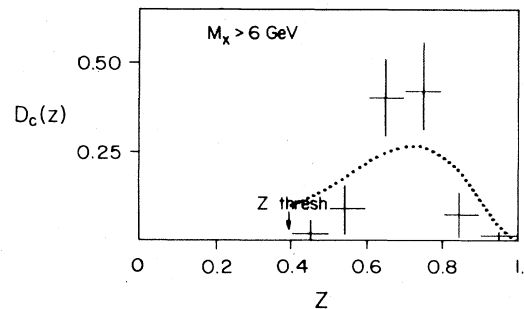


FIG. 13. Distribution of  $z = 2E_{D^*}/M_X$  for  $D^*$  events with  $M_X > 6$  GeV. Dotted curve is a fit to the form suggested in Ref. 31 with  $\epsilon = 0.11$  (Ref. 30).

described above. A small part of the resulting distribution in  $M_Z^2$  around zero is shown in Fig. 12 with the Monte Carlo expectation for  $D^*\bar{D}^*$  only events. The dotted line contains 95% of Monte Carlo events and, at 90% C.L., < 18% of the data. In summary, all four measurements are consistent with the  $M_Y^R$  based result that only  $(11 \pm 7)\%$  of  $D^*$  are accompanied solely by a  $\bar{D}^*$  or a  $\bar{D}$ . In  $e^+e^- \rightarrow D + \text{anything}$  at  $E_{\text{c.m.}} = 5.2$  GeV the Mark II group at SPEAR has made a similar observation that most of  $D$  production is not quasi-two-body.<sup>26</sup>

The distribution of  $z = 2E_{D^*}/M_X$  in the  $M_X$  center of mass is shown for  $D^*$  events in Fig. 13. This is a measurement of the charm-fragmentation function modified by threshold effects which we have attempted to reduce by cutting the data at  $M_X > 6$  GeV. The  $D^*$  events are concentrated near  $z=0.7$ . Similar results have been seen in neutrino,<sup>27</sup> muon,<sup>28</sup> and  $e^+e^-$  (Ref. 29) interactions. The curve is a fit<sup>30</sup> to this earlier data using the parameterization developed by Peterson *et al.*<sup>31</sup>

The distributions of Feynman  $x$  in the overall c.m. for the  $D^*$ 's, for all events, and for single-recoil-proton events are shown in Fig. 14. We have fitted both distributions to the form  $a(1-x_F)^n$  and obtained the values of  $n=0.7 \pm 0.4$  and  $1.1 \pm 0.4$ , respectively. A similar value of  $n \approx 1$  was also observed for pions produced in single-proton events.<sup>11</sup>

Finally, we have also addressed the question of the importance of associated production processes in  $D^*$  photoproduction. We have used  $D^{*\pm}$  events obtained with the  $\Lambda_c$  sensitive trigger to look at the  $\bar{D}^*-D^*$  charge asymmetry. In the  $K\pi$  mode the difference is  $6 \pm 5$  events, while in the  $K\pi\pi^0$  mode it is  $13 \pm 11$  events. (In the high-mass diffractive trigger, the corresponding values are

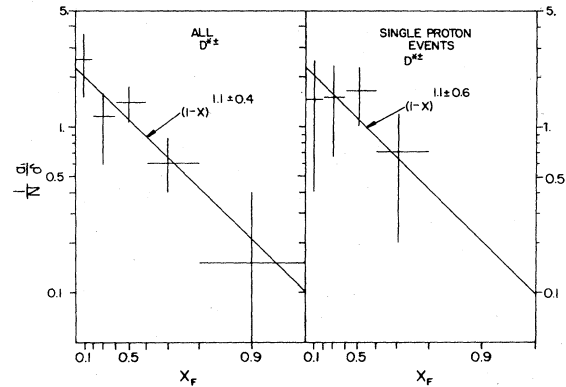


FIG. 14. Distributions of  $D^*$  Feynman  $x$  for all events and for single-recoil-proton events. Results of the fits to the form  $a(1-x_F)^n$  are superimposed.

$-10 \pm 8$  and  $25 \pm 11$  events.) Interpreting the asymmetry as coming entirely from the associated production process we obtain, after correcting for trigger and reconstruction efficiencies,<sup>32</sup> an upper limit for the cross section  $\sigma(\gamma p \rightarrow (\bar{D}^{*-} + \text{anything})\Lambda_c) < 60$  nb (90% C.L.) with an additional 40% uncertainty in the absolute normalization.

We wish to acknowledge the assistance of the staff of Fermilab (in particular that of the Physics and Proton Area Departments) and the technical support staffs of all the university groups involved. This research was supported by the U.S. Department of Energy and by the Natural Science and Engineering Research Council of Canada through the Institute of Particle Physics of Canada and the National Research Council of Canada.

(a)Present address: Comavid Corporation, North Aurora, Illinois.  
 (b)Present address: University of California, San Diego, California.  
 (c)On sabbatical leave from National Institut voor Kernfysica en Hige-Energiefysica, NIKHEF-H, Amsterdam, The Netherlands.  
 (d)Present address: University of California, Berkeley, California.  
 (e)Present address: University of Oklahoma, Norman, Oklahoma.  
 (f)Present address: University of California, Irvine, California.  
 (g)Present address: Institute for Research at Particle Accelerators, Palo Alto, California.  
 (h)Present address: California State University, Northridge, California.  
 (i)Present address: University of Washington, Seattle, Washington.  
 (j)Present address: Bell Laboratories, Allentown, Pennsylvania.  
<sup>1</sup>M. A. Shifman, A. I. Vainstein, and V. I. Zakharov, Phys. Lett. **65B**, 255 (1976).  
<sup>2</sup>J. Babcock, D. Sivers, and S. Wolfram, Phys. Rev. D **18**, 162 (1978).  
<sup>3</sup>H. Fritsch and K. H. Streng, Phys. Lett. **72B**, 385 (1978).  
<sup>4</sup>F. Halzen and D. M. Scott, Phys. Lett. **72B**, 404 (1978).  
<sup>5</sup>L. M. Jones and H. W. Wyld, Jr., Phys. Rev. D **1**, 2332 (1978).

<sup>6</sup>M. Gluck and E. Reya, Phys. Lett. **79B**, 453 (1978).  
<sup>7</sup>T. Nash, in *Proceedings of the International Symposium on Lepton and Photon Interactions at High Energies, Ithaca, New York*, edited by D. G. Cassel and D. L. Kreinick (Newman Laboratory of Nuclear Studies, Cornell University, Ithaca, 1983).  
<sup>8</sup>A. R. Clark *et al.*, Phys. Rev. Lett. **45**, 682 (1980).  
<sup>9</sup>J. Aubert *et al.*, Nucl. Phys. **B213**, 1 (1983); **B213**, 31 (1983).  
<sup>10</sup>M. Binkley *et al.*, Phys. Rev. Lett. **50**, 302 (1983); NA14 Collaboration Report No. 83-0734 (unpublished); contributed paper to the International Symposium on Lepton and Photon Interactions at High Energies, Ithaca, New York.  
<sup>11</sup>The spectrometer is described in detail in A. Duncan, Ph.D. thesis, University of Colorado, 1982; B. H. Denby, Ph.D. thesis, University of California, 1983; D. J. Summers, Ph.D. thesis, University of California, 1984.  
<sup>12</sup>D. J. Summers *et al.*, Phys. Rev. Lett. **52**, 410 (1984).  
<sup>13</sup>B. H. Denby *et al.*, Phys. Rev. Lett. **52**, 795 (1984).  
<sup>14</sup>V. K. Bharadwaj *et al.*, Nucl. Instrum. Methods **228**, 283 (1985).  
<sup>15</sup>J. A. Appel *et al.*, Fermilab Report No. FN-405, 2125.000, 1984 (unpublished).  
<sup>16</sup>G. Hartner *et al.*, Nucl. Instrum. Methods **216**, 113 (1983).  
<sup>17</sup>E. Barsotti *et al.*, IEEE Trans. Nucl. Sci. **NS-26**, 686 (1979); J. Martin *et al.*, in *Proceedings of the Topical Conference on the Application of Microprocessors to High Energy Experi-*

- ments (Report No. CERN 81-07, 1981), p. 164; T. Nash, *ibid.*, p. 132.
- <sup>18</sup>S. Bhadra, Ph.D. thesis, University of Colorado, 1985.
- <sup>19</sup>G. Trilling, Phys. Rep. **75**, 177 (1981).
- <sup>20</sup>Particle Data Group, Phys. Lett. **111B**, 1 (1982).
- <sup>21</sup>Figure taken from Ref. 7; data come from Refs. 8, 9, 22, and Stanford Linear Accelerator Center Hybrid  $\gamma$  Collaboration, K. Abe *et al.*, Phys. Rev. Lett. **51**, 156 (1983); J. C. Kent, Ph.D. thesis, Berkeley, 1983; Omega Spectrometer ( $\Omega$ ) Collaboration, D. Aston *et al.*, Phys. Lett. **94B**, 113 (1980).
- <sup>22</sup>M. S. Atiya *et al.*, Phys. Rev. Lett. **43**, 414 (1979); P. Avery *et al.*, *ibid.* **44**, 1309 (1980).
- <sup>23</sup>J. D. Bjorken, in *Proceedings of the SLAC Summer Institute on Particle Physics, 1973*, edited by M. C. Zipf (SLAC, Stanford, 1973) (SLAC, Report No. 167), Vol. 1, p. 1; J. D. Bjorken, Phys. Rev. D **17**, 171 (1978).
- <sup>24</sup>See, e.g., S. F. King, A. Donnachie, and J. Randa, Nucl. Phys. **B167**, 98 (1980).
- <sup>25</sup>P. Avery, Ph.D. thesis, University of Illinois, 1980; also P. Avery *et al.*, Phys. Rev. Lett. **44**, 1309 (1980).
- <sup>26</sup>M. W. Coles *et al.*, Phys. Rev. D **26**, 2190 (1982).
- <sup>27</sup>CERN-Dortmund-Heidelberg-Saclay Collaboration, H. Abramowicz *et al.*, Z. Phys. C **15**, 19 (1982); N. Ushida *et al.*, Phys. Lett. **121B**, 292 (1983).
- <sup>28</sup>References 8 and 9.
- <sup>29</sup>J. Yelton *et al.*, Phys. Rev. Lett. **49**, 430 (1982); C. Bebek *et al.*, *ibid.* **49**, 610 (1982); TASSO Collaboration, M. Althoff *et al.*, Phys. Lett. **126B**, 493 (1983); **130B**, 463(E); CLEO Collaboration, P. Avery *et al.*, Phys. Rev. Lett. **51**, 1139 (1983).
- <sup>30</sup>K. Kleinknecht and B. Renk, Z. Phys. C **17**, 325 (1983).
- <sup>31</sup>C. Peterson *et al.*, Phys. Rev. D **27**, 105 (1983).
- <sup>32</sup>A quasi-two-body Monte Carlo model was used to estimate the trigger efficiency for the process  $\gamma p \rightarrow (\bar{D}^{*-} + \text{anything})\Lambda_c$ . A  $t$  distribution of the form  $\exp(-2|t|)$  was assumed, and  $\Lambda_c$  was allowed to decay into 40 modes. Assuming reasonable branching ratios we estimate the trigger efficiency to be  $(15 \pm 5)\%$ . The forward spectrometer efficiency was estimated using Monte Carlo events with a single  $D^*$  and, on average, two additional pions in the forward system.